NRC Research Press

ARTICLE

Evaluating the effect of seismic surveys on fish — the efficacy of different exposure metrics to explain disturbance

Nils Olav Handegard, Tron Vedul Tronstad, and Jens Martin Hovem

Abstract: To assess potential disturbance effects on fish from seismic air-gun surveys, we described several metrics to characterize the exposures from such surveys, including the number of emissions by area and time, and metrics based on accumulated sound exposure levels (SEL). For the SEL-based metrics we used both a simple spherical–geometrical model and a model that incorporated physical sound propagation properties such as bottom topography and the vertical difference in sound speed. We applied the metrics to two experiments in Norwegian waters (the Nordkappbanken and Vesterålen experiments) where fish distributions and fisheries were affected by the air-guns, but where the disturbance was stronger in the Nordkappbanken case. The metrics based on the number of emissions by area and time showed a stronger impact in the Nordkappbanken case. For the SEL-based metrics, the simple sound propagation model failed because of artificially elevated levels close to the emissions, but for the more complex propagation model, contrary to expectations, a stronger SEL was found in the Vesterålen case. We conclude that simple sound propagation models should be avoided and that the reliance on sound energy metrics like SEL for disturbance effects must be interpreted with caution.

Résumé : Dans le but d'évaluer les possibles effets que peuvent avoir les échantillonnages sismiques par canons à air, nous décrivons différentes métriques permettant de caractériser l'exposition de telles pratiques d'échantillonnage. Ceci inclut le nombre d'émissions par zones et périodes ainsi que les métriques basées sure les niveaux accumulés d'exposition sonore (SEL). Nous avons utilisés deux modèles distincts de propagation du son. En particulier, le second modèle intègre les propriétés physiques de la propagation du son comme la topographie ou la différence verticale de vitesse du son. Nous avons appliqué les métriques à deux études lors lesquelles les distributions des poissons ainsi que le succès de pêche ont été affectés. Le niveau de perturbation reporté était plus important lors de la première étude. Les métriques basées sur le nombre d'émissions en fonction de la zone et de la période montrent une exposition sonore plus forte lors de la première étude. Pour les métriques basées sur les SEL, si le modèle de propagation simple du son n'apparait pas satisfaisant du fait de niveaux artificiellement élevés proche de la source d'émission, le second modèle de transmission, et ce contrairement à nos attentes, détecte un SEL plus fort lors de la seconde étude. Nous concluons que les modèles de propagation simple du son ne devraient pas être employés et que l'utilisation de métriques tel que le SEL pour des effets de perturbation se doivent d'être interprétés avec précaution.

Introduction

Geological (air-gun) surveys map the sub-bottom structures of the sea floor and are used extensively for locating petroleum resources. The air-gun arrays are designed to create an acoustic pulse that penetrates the sea floor, but parts of the pulse also radiate horizontally into the water column. Air-guns contribute to increased anthropogenic noise in the oceans (Hildebrand 2009), and there are growing concerns that increased aquatic noise pollution may have detrimental effects on aquatic life (Slabbekoorn et al. 2010).

Air-gun emissions have caused behavioural changes in caged fish (Pearson et al. 1992; Hassel et al. 2004), damaged the fish auditory system (McCauley et al. 2003), and generated large-scale changes in horizontal (Engås et al. 1996) and vertical (Slotte et al. 2004) fish distributions. Changes in catch per unit effort have also been observed for fisheries in close proximity to seismic surveys (Skalski et al. 1992; Engås et al. 1996; Løkkeborg et al. 2012). Concerns about the effect of noise on aquatic life are finding their way into policy documents, such as the EU marine strategy framework directive (Anonymous 2012).

Several exposure metrics can be used to characterize the impact of air-gun surveys. These include simple metrics such as number of air-gun emissions within an area or time interval or metrics based on the actual energy or other properties of the air-gun emissions. Sound pressure level is often used to characterize sound, but this is misleading for transient air-gun emissions, as it relies on the root mean square pressure over an unspecified averaging window (Madsen 2005). Appropriate measures for transients are defined in the ANSI standard for measurement of impulse noise (Anonymous 1986) and include peak-to-peak pressure, rise time, impulse, a-duration, etc. A useful metric for transients is the sound exposure level (SEL). This is a measure of energy in a pulse (Carey 2006) and can be summed across emissions to give an overall measure of sound energy over a certain period of time, such as daily or total exposure doses, similar to noise dose estimation for humans (Heathershaw et al. 2001).

Two large-scale experiments on the effect of seismic surveys have been conducted off the northern Norwegian coast (Table 1; Fig. 1) and used as cases in this study: the Nordkappbanken experiment (Engås et al. 1996) and the Vesterålen experiment (Løkkeborg et al. 2012). Both experiments assessed the impact of seismic surveys on fisheries and investigated changes in fish

Received 24 October 2012. Accepted 30 May 2013.

Paper handled by Associate Editor Josef Michael Jech.

N.O. Handegard. Institute of Marine Research, P.O. Box 1870 Nordnes, 5817 Bergen, Norway.
T.V. Tronstad. SINTEF, Postboks 4760 Sluppen, 7465 Trondheim, Norway.
J.M. Hovem. SINTEF, Postboks 4760 Sluppen, 7465 Trondheim, Norway, and NTNU, Institutt for elektronikk og telekommunikasjon, 7491 Trondheim, Norway.
Corresponding author: Nils Olav Handegard (e-mail: nilsolav@imr.no).

Table 1. The key differences between the two experiments, including the different air-gun configurations.

	Unit	Vesterålen	Nordkappbanken
Duration	Days	37.7	4.73
Exposures (count)	—	164 000	27 000
Area	n.mi.^{2}	368	30
Exposures per duration	Days^{-1}	4 349	5 706
Exposures per area	n.mi.$^{-2}$	446	901
Exposures per duration and area	n.mi.$^{-2}$ Days^{-1}	11.8	190
Active guns (count)	—	34	18
Air-gun pressure	kPa	13 784	13 784
Total active volume	L	57	82

Note: 1 nautical mile (n.mi.) = 1.853 km; 13 784 kPa = 2000 psi.

distributions before, during, and after the exposure. In the Nordkappbanken experiment, trawl catches of Atlantic cod (*Gadus morhua*) and haddock (*Melanogrammus aeglefinus*) and long-line catches of haddock were reduced by 70% within the exposure area (5.5 km × 18.5 km). The reduced catches were confirmed by an acoustic echo-integration survey. For the larger exposure area (14 km × 85 km) in the Vesterålen experiment, gill-net catches of redfish (*Sebastes norvegicus*) increased by 86% and Greenland halibut (*Reinhardtius hippoglossoides*) by 132%, while 25% and 16% reductions in long-line catches of haddock and Greenland halibut, respectively, were reported. The increased gill-net catches were explained by a change in swimming pattern that lead to increased encounters with gill nets. There was also a general reduction in catch rates for other species. However, except for haddock, no difference was found by the acoustic survey, and no changes in the behaviour of Atlantic herring (*Clupea harengus*) schools were found when tracking the exposed schools using fisheries sonar (Peña et al. 2013). In summary, the level of disturbance was less than for the Nordkappbanken experiment, and the authors concluded that "less intense sound exposure compared with previous studies and strong habitat preference in some species may explain this finding" (Løkkeborg et al. 2012).

The objective of this work is to apply the exposure metrics to the two experiments and to assess their performance. The overall level of disturbance was less in the Vesterålen experiment, and we expect this to be reflected in the exposure metrics. It is worth noting that the experiments were different in a multitude of aspects, but the rationale for addressing the noise exposure metrics is their increasing role in policy documents and regulations.

Materials and methods

We used several metrics to characterize the noise exposures for the two experiments. These included simple metrics such as number of exposures by area and time and energy (SEL)-based metrics derived from two different propagation models: a simple combination of spherical and cylindrical transmission loss and a ray-tracing model that incorporated seafloor structures and sound speed gradients in the water column. For the SEL-based metrics we defined a central point of interest, denoted $\boldsymbol{x}$, within each survey area where we calculated the metrics (Fig. 1). In general, any location of interest could be defined, such as to match a fishing activity, a central position in the exposure area, or even moving points in space to match animal movements.

Seismic surveys and physical sound propagation properties

The positions of the air-gun emissions were required for the metrics. In addition, the SEL-based metrics required the configuration of the air-gun cannons, the sound speed profiles, and bottom topography.

The seismic exploration vessel RV *Academic Skatskiy* was used for the Nordkappbanken experiment. The positions of each air-gun emission, $\boldsymbol{x}_i'$, were estimated from the description of the experiment (Engås et al. 1993, their appendix D). The positions are given in Euclidean distance relative to the reference position (72°20′N, 26°00′E), while the index i denotes the individual air-gun emission. In the Vesterålen experiment, the seismic exploration was done by RV *Geo Pacific*, and geo-referenced positions from the surveyor's log files were converted to Euclidean distance relative to the reference position (69°10.1′N, 14°37.4′E). The configurations of the air-guns for the two experiments are given in Table 1.

The vertical sound speed profiles were calculated using the Del Grosso equation (Del Grosso 1974) from conductivity, temperature, and depth (CTD) profiles taken in the survey areas. For the Nordkappbanken experiment, a portable CTD (Gytre 1991) was used, and for the Vesterålen experiment, a Seabird SBE911 CTD was used. Stratification was stronger in the Vesterålen case than for the Nordkappbanken case (Fig. 2*a*).

The bottom topography and substrate are important parameters for sound propagation. In the Nordkappbanken experiment, the acoustic survey vessel's echosounder was used to measure the depths in the area. The bottom was almost flat with approximately ±5 m variation over the whole exposure area (Fig. 2*b*). The bottom substrate consisted of sand and sandy mud (Anonymous 2013). The simulations assumed that the grain size was approximately 63 μm, giving a density of 1700 kg·m^{-3}, compressional wave speed of 1620 m·s^{-1}, shear wave speed of 500 m·s^{-1}, compressional wave attenuation of 0.1 dB·m^{-1}, and shear wave attenuation of 0.3 dB·m^{-1} (Hamilton 1987).

In the Vesterålen experiment the bottom topography varied substantially across the exposure area. The bottom topography data was available from the surveyor's log files, but only along a subset of lines in the northeast direction (Fig. 1*b*). The bottom substrate varied from sand to gravel, cobbles, and boulders, but the majority of the area was gravel. This gave a density of 2500 kg·m^{-3}, compressional wave speed of 2000 m·s^{-1}, shear wave speed of 600 m·s^{-1}, compressional wave attenuation of 0.1 dB·m^{-1}, and a shear wave attenuation of 1 dB·m^{-1} (Hamilton 1987).

Simple noise propagation model

The simple noise propagation model assumes a combination of spherical and cylindrical transmission loss to calculate the SEL for each emission. At close range, typically in the same order of magnitude as the bottom depth, free field approximations may be appropriate and lead to a spherical transmission loss. For ranges greater than the bottom depth, an ideal waveguide with perfectly reflecting boundaries can be assumed, which results in a cylindrical spreading loss. A combination of the two is expressed by

$$E_i = E^{(0)}\left(\frac{r_i}{r_0}\right)^{-2}\left(1 + \frac{r_i^2}{r_t^2}\right)^{\frac{1}{2}} \quad (1)$$

where $E^{(0)}$ is the sound exposure extrapolated to the reference distance $r_0 = 1$ m, $r_i = |\boldsymbol{x}_i' - \boldsymbol{x}|$, and r_t is the transition range, usually close to the water depth. The energy flux density source level (Carey 2006) referred to a distance of 1 m is defined as

$$\mathrm{EFSL} = 10\log_{10}\left[\frac{E^{(0)}}{E_{\mathrm{ref}}}\right]\mathrm{dB\ re\ 1}\mu\mathrm{Pa}^2\ (1\ \mathrm{s}) \quad (2)$$

where E_{ref} is the reference level. Note that Carey (2006) uses the notation E_x as opposed to E. Note also that source levels are different than the actual exposure level close to the air-gun (Caldwell and Dragoset 2000), since the signals from the individual air-guns interact and create the combined and focused pulse in the far field. Consequently, the EFSL serves only as a reference when estimating the levels at a distance and are not valid at short range.

Fig. 1. (*a*) The locations of the two case studies; (*b*) and (*c*) denote the locations of the Nordkappbanken and Vesterålen experiments, respectively. (*b*, *c*) The gray areas indicate the positions of the seismic air-gun emission shots, and "+" indicates the middle positions for each area chosen as the position of interest **x**. (*c*) The solid line indicates the modelled exposure transect.

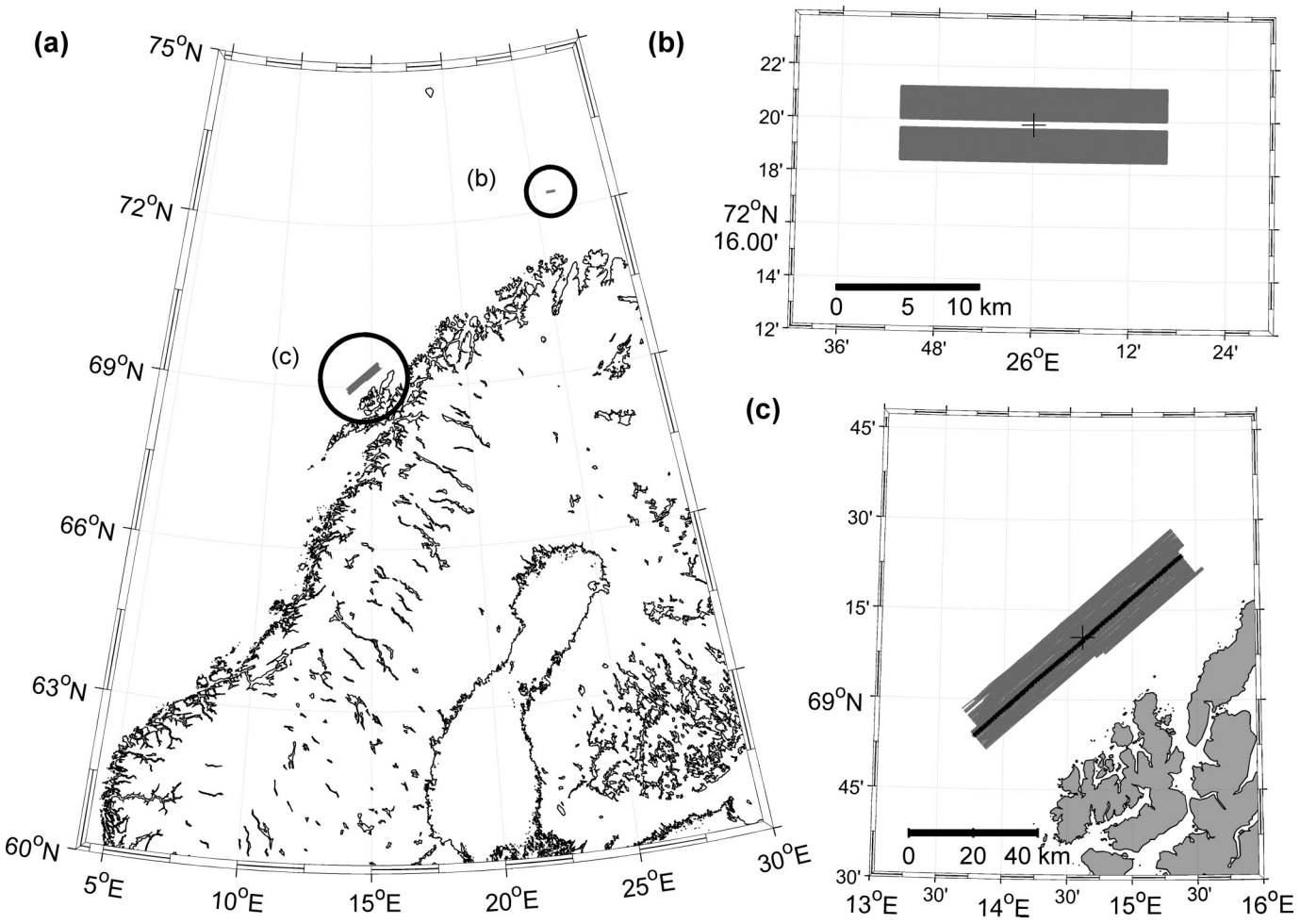

For the Vesterålen experiment, noise observations were available (Fig. 3; Løkkeborg et al. 2010). The measurements were obtained using a free-floating buoy, containing three Naxys 02345 Ethernet hydrophones (Naxys, Bergen, Norway), positioned at 8, 32, and 64 m depth, and the model could be fitted directly to the hydrophone measurements. Assuming that r_t = 135 m, which is the approximate bottom depth at the location of the buoy, we can fit eq. 1 to the observations (Fig. 3). The estimated EFSL from the hydrophone using eq. 1 is then 250.5 dB re 1 μPa² (1 s). For the Nordkappbanken experiment, we did not have hydrophone observations and simply used the same source level of 250.5 dB as in the Vesterålen case. Note that no difference in directionality was assumed and that the air-gun configuration was slightly different; based on the data in Table 1 and following Caldwell and Dragoset (2000), we may expect a difference of 1.3 dB re 1 μPa² (1 s). Using eq. 1 we can then obtain estimates of SEL at any distance from the source, which were then used to estimate the daily exposure at the position of interest.

Ray-tracing propagation model

Noise propagation is far more complex than the simple model described above and includes multipath reflections from the surface, bottom, and ray bending, interactions with the bottom substrate, etc. The different propagation paths may converge in zones to give highly elevated levels at larger distances (Hovem et al. 2012). Based on the available data, a full 4D propagation model would be too complicated, and as a compromise we used a 2D ray-tracing model ("PlaneRay"; Hovem 2011; Tronstad and Hovem 2011; Hovem et al. 2012). For an overview of other models and for further references, see Jensen et al. (2011).

In the simulations, the air-gun array was placed 6 m deep, and the model found the trajectories, travel times, and amplitudes of the rays along the bathymetry lines (Figs. 1, 2*b*) and calculated the SEL at various depths by coherent addition of the multiple arrivals at any depth and distance away from the source. No rays were traced into the bottom; rather, the bottom interaction was described by plane-wave reflection coefficients of the bottom layer using sound speed and density for the two locations as described above, including the effect of varying bottom topography (Fig. 2*a*). The speed of sound varied with depth only, and the sound speed profiles based on the observations were used in the simulations (Fig. 2*a*). We used a simplified model for the vertical directionality (Hovem et al. 2012).

The model was set up to estimate the weighted SEL for two different depth distributions: the near bottom estimate (*B*) centred at 10 m from bottom (σ = 10 m) and a pelagic estimate (*P*) centred at 30 m depth (σ = 10 m). Both estimates weighted the depth-distributed SEL from the model with a Gaussian weight function with σ as the standard deviation. The model was evaluated using the same noise observations as for the simple case described above.

For the Nordkappbanken experiment, the SEL estimates at the point of interest **x** for each emission pulse was straightforward.

Fig. 2. (*a*) Sound speed profiles from the Nordkappbanken and Vesterålen experiments, shown on the left and right, respectively. The mean sound speed profiles used in the simulations are given as black lines, and the sound speed for each conductivity–temperature–salinity profile is given as gray lines. For the Vesterålen experiment, the sound speed profile is extrapolated below 250 m. (*b*) The bottom topography along the transect from Vesterålen is shown as a black line. For the Nordkappbanken experiment, the depth is assumed constant at 247 m (dashed straight line). The distance $r' = 0$ is the point along the transect closest to the point of interest $\boldsymbol{x}$.

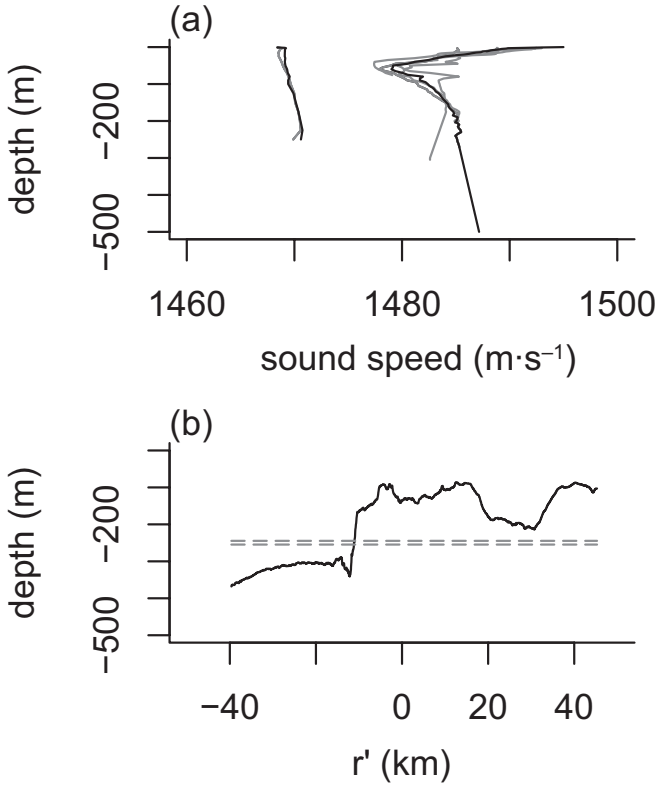

Since the bottom was flat, the SEL was simply found by looking up SEL for a given range r' away from the source, ignoring the direction. Note that this assumes no horizontal directionality. In this case, $r' = r_i$ and $r_i = |\boldsymbol{x}_i' - \boldsymbol{x}|$ (cf. Fig. 4*a*). The Vesterålen experiment was more complicated, since the modelled line was only representative for that particular topography line. However, most of the exposures were along the northeast direction and at a distance away from the point of interest, and the path was for the most part along similar bottom topography. As an approximation we assumed that the modelled line was representative of the distance between the point of interest $\boldsymbol{x}$ and the air-gun emission $\boldsymbol{x}_i'$. We projected $\boldsymbol{x}$ on to the modelled transect ($r' = 0$, cf. Fig. 4*a*), and the model estimated the SEL as a function of distance r' from the projected point. Again, assuming no horizontal directionality and relying on the predominant norhteast direction, we approximated the SEL for a given emission by setting $r' = r_i$, where r_i is simply the distance between the point of interest and the emission (Fig. 4).

Noise dose

Since the SEL, as defined here, contained the energy in a single pulse, the total energy at a given location of interest $\boldsymbol{x}$ over a specific time period could be found by summing the contributions from all air-gun emissions. In this paper we have used a 24 h accumulated SEL, which is similar to the noise dose used for human noise regulations (Heathershaw et al. 2001), except that it

Fig. 3. (*a*) Noise observations taken from Løkkeborg et al. (2010). The hydrophones were positioned at 32, 73, 184, and 383 m depth, and the gray lines show the SEL from each hydrophone where increasingly dark curves indicate deeper hydrophones. Two lines are shown for each depth, since both the approach and departure of the seismic vessel is included. The dashed black curve is the simple transmission model based on fitting the model to the observations. (*b*, *c*) The modelled SEL as a function of distance r' along the modelled transect for the Nordkappbanken (*b*) and the Vesterålen (*c*) experiments. The dashed, grey, and solid black lines are the simple model, the pelagic estimates, and the bottom related estimates, respectively.

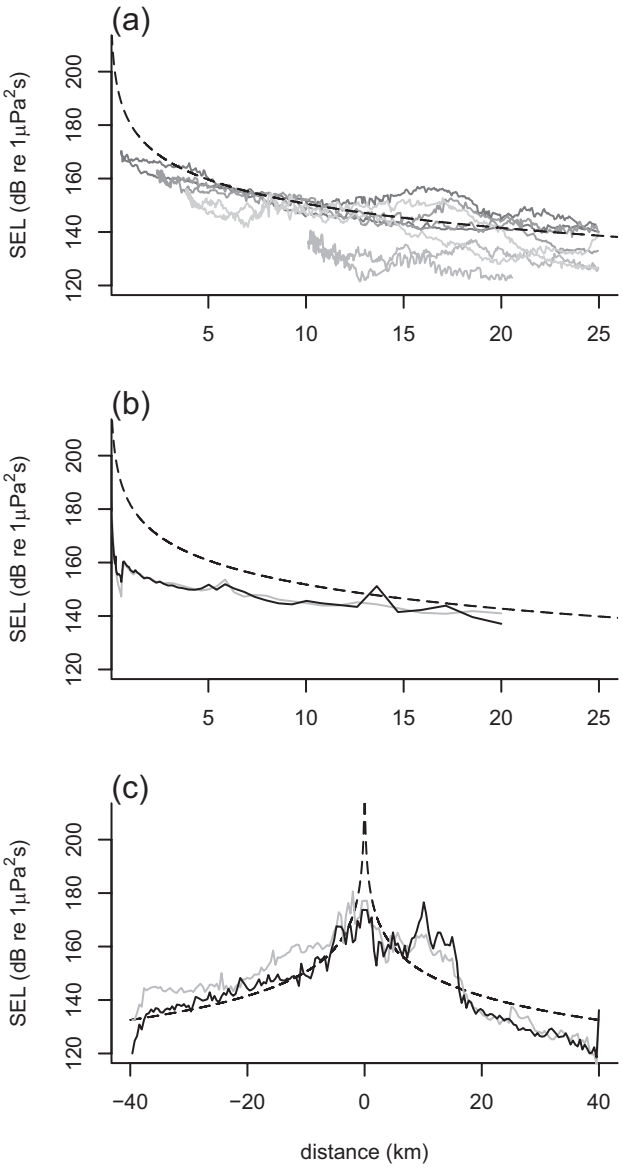

is not scaled by the 8 h exposure time convention. The 24 h cumulative sound exposure level D_k at the location of interest $\boldsymbol{x}$ for day k was found by summing the exposure from all seismic emissions within 24 h for the day in focus:

$$D_k = 10\log_{10}\left[\frac{\sum_{i\in A_k} E_i}{(1\ \mu\text{Pa}^2)(1\ \text{s})}\right] \quad (3)$$

where A_k is the set of air-gun emissions i within each day k, and E_i is the exposure from each air-gun emission i, which can be the

Fig. 4. (*a*) Schematic showing the projection (dashed line) of the point of interest $\boldsymbol{x}$ onto the model line defining $r' = 0$ and how $r' = r_i$ is defined as the distance between the seismic emission $\boldsymbol{x}_i'$ and the point of interest $\boldsymbol{x}$. (*b*, *c*, *d*) The Nordkappbanken and Vesterålen experiments are shown as broken and solid lines, respectively. The solid black and grey curves are the bottom and surface related estimates, respectively. (*b*) The number of air-gun emission for different ranges. (*c*) The daily dose for the central position $\boldsymbol{x}$. The bottom and surface related estimates are almost indistinguishable for the Nordkappbanken experiment and are plotted as a single dashed line. The horizontal lines to the right in the panel show the total summed dose over the full duration of the experiment. (*d*) The percentages of the total SEL contribution by range.

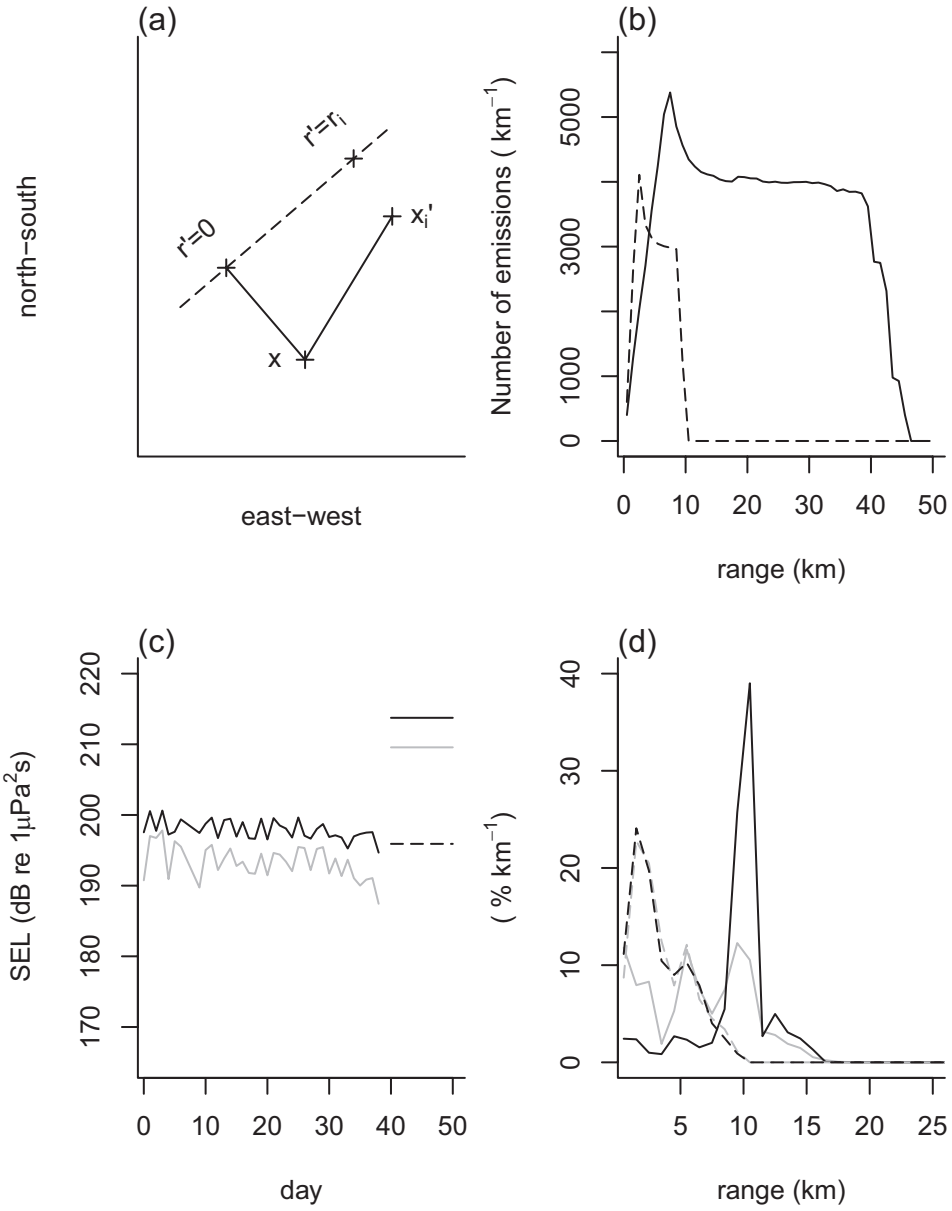

output from both the simple model and the ray-tracing model. In addition to binning the air-gun emissions by day, we also binned the emissions by range. This gave the total energy from exposures at a given range and was used to provide information about the distances that contributed to the exposures.

Results

The simple picture — the number of exposures by distance, area, and time

Key sound exposure metrics were different between the experiments (Table 1). The duration of the Vesterålen experiment was approximately eight times longer than the Nordkappbanken experiment, but the number of exposures per unit time was approximately 30% higher. Further, in the Vesterålen experiment the cumulative energy was distributed over an area one order of magnitude larger. The exposures per area and unit time were 16 times higher for the Nordkappbanken experiment. These indicate a larger fish disturbance on the smaller area when using these simple metrics, which was in accordance with our expectations of a stronger fish reaction and distribution change for that case.

The exposures at the central position, $\boldsymbol{x}$, within the survey (Fig. 1) was calculated. The distribution of distances between the point of interest and positions of the air-gun emissions, given by the distribution of $r_i = |\boldsymbol{x}_i' - \boldsymbol{x}|$, gave an indication of the distances between the seismic vessel and the position of interest throughout the experiments. This gave an indirect indication of the noise

energy exposure (Fig. 4*b*). There were a higher number of exposures from short ranges for the Nordkappbanken experiment.

Sound exposure levels

For both models and both experiments, the SEL estimates were modelled as a function of distance r' (Fig. 3) along the topography transects (Fig. 2), while the ray-tracing model estimated the SEL for two different depths. The simple model gave highly elevated levels close to the source, while the ray-tracing model did not. For the Nordkappbanken experiment, the sound speed increased slightly with depth over the whole water column (Fig. 3), causing the rays to bend upwards towards the sea surface and creating weak convergence zones at ranges of 12, 24, and 36 km and deep convergence zones at about 125 m depth. The rays to these zones did not interact with the bottom, and sound in these zones was therefore independent of the bottom structure, but somewhat dependent on sea surface conditions as the rays struck the surface. For the Vesterålen experiment, nearly all of the acoustic energy was transmitted via bottom- and surface-reflected paths. This meant that the properties of the sea surface and, in particular, the bottom were important.

Daily total energy exposure

The daily accumulated SEL (dose) for each experiment and the accumulated dose for the duration of the experiment are given in Fig. 4*c*. The daily dose from the simple model was sensitive to the choice of central position and was substantially higher (~20 dB) because of the artificially elevated levels close to the source. For this reason we omitted the results from this model in the daily exposure results.

The surprising result was that the daily dose estimates from the Nordkappbanken experiment were **less** than those from the Vesterålen experiment. This resulted in the total exposure, even if the Nordkappbanken experiment was intense, being lower. This was contrary to the signal from the simple metrics.

To understand this, it is informative to know how transmissions at a given range contributed to the total sound exposure. To do that, we binned the SEL into range bins away from the central position and summed the contribution at each range. This gave an estimate of how much of the total exposed energy was obtained from different ranges (Fig. 4*d*). In the Nordkappbanken experiment, the contribution to the total exposure was dominated by exposures at relatively close range, whereas for the Vesterålen experiment the contribution was dominated by contributions from around 10 km. This was a combination of the distance distribution to the emissions and the sound propagation effects. For the SEL based on the simple transmission model (eq. 1), 98% and 62% of the total exposure came from the first kilometre for Nordkappbanken and Vesterålen, respectively, which was an artefact of the artificially elevated levels at close range. This illustrates a potential pitfall of using simple models when estimating sound exposure.

Discussion

The objectives at the outset of this work were to use exposure metrics to characterize the effect of air-gun emissions on fish from the two experiments and to assess the efficacy of these exposure metrics to explain the differences in responses. The simple metrics, such as exposures per area, fitted well with our initial expectation that there should be a higher impact in the smaller Nordkappbanken area. However, when modelling the SEL, the results did not support these expectations.

When computing the SEL for the two experiments, we made a series of simplifications. The simple model disregarded the topography and the physical environment and provided a crude estimate. Since the main contribution to the noise dose occurred at short distances (cf. Fig. 4*d*), short-range performance of the model is particularly important for obtaining reliable SEL estimates. Several simplifications were also made for the ray-tracing model. These included using just one modelled shooting line as being representative of the whole area, disregarding the horizontal directivity pattern, and assuming similar source levels and vertical directivity for the two experiments. Regardless of these simplifications, the improved performance at close range and the importance of the bottom topography in the Vesterålen experiment highlights the deficiencies of simple propagation models when estimating SEL.

In the Introduction we alluded to the notion that the two experiments were different in a wide range of aspects and that it was perhaps naive to expect that the difference in disturbance could be explained solely by the accumulated SEL. In general, fish reactions to anthropogenic disturbances have been shown to resemble predator avoidance reactions (Frid and Dill 2002), and several studies have demonstrated how the internal state of an organism or its environment may affect the threshold for responding to a perceived threat (e.g., Milinski et al. 1990; Lima and Dill 1990). We have only used two cases in this paper, and it is not possible to attribute the difference in reaction to a single explanation such as "the fish were feeding" or "the fish were migrating". However, they do illustrate how potential trade-offs may change the response of fish to a disturbance and how important it is to report the general situation and state of the fish in such a study. A more extensive discussion can be found in a review of fish response to vessels noise (De Robertis and Handegard 2013). Consequently, the link between disturbance stimuli (here in terms of accumulated SEL) and response should not necessarily be expected to be linear.

Our approach addresses sound exposure on an emission by emission scale, and it may be worth relating this approach to that of other spatial scales. At short range the energy from the air-guns can cause hearing loss or physical injury (Popper and Hastings 2009). However, it has been indicated that freely moving fish can move out of the area of such impact (McCauley et al. 2003). At larger scales than we considered here (more than 40 km), the air-guns may contribute to a general increase in background noise (Hildebrand 2009). For management purposes these long-range effects may be important, since the area of impact is larger. This paper addresses the medium-range effects (between hearing loss and effects of increased background levels) and should be interpreted in that context.

From testing the various metrics on the two cases, we can conclude that one should be cautious when using simple metrics such as exposures by area and time as a proxy for disturbance. Furthermore, when SEL is calculated, simple transmission models may be misleading, particularly at short ranges, and we recommend using more realistic models that incorporate properties of the physical environment. This is clearly demonstrated when we apply the results to our two cases, where it has been assumed that the difference in response was attributed to the higher disturbance in the Nordkappbank case. Consequently, caution needs to be exercised when relying on SEL as an impact indicator, since there is not necessarily a clear link between sound energy and disturbed behaviour. However, even if a linear response to the disturbance was established, it is important to acknowledge that the long-term consequences for fish population dynamics and fisheries, which are relevant for management, will still be unclear.

Acknowledgements

This work was partially financed by the Norwegian Ministry of Fisheries through the Institute of Marine Research "Oil and Fish programme" (NOH), the Norwegian Research Council (NOH and JMH, grant 204229/F20), and SINTEF (TVT). The comments of Alex De Robertis, Gavin J. Macaulay, and Guillaume Rieucau improved the paper.

References

Anonymous. 1986. American National Standard: Methods for measurements of impulse noise. ANSI S12.7-1986 (R2006).

Anonymous. 2012. Directive 2008/56/EC of the European Parliament and of the Council of 17 June 2008 establishing a framework for community action in the field of marine environmental policy (Marine Strategy Framework Directive) (Text with EEA relevance) [online]. Available from http://eur-lex.europa.eu/LexUriServ/LexUriServ.do?uri=CELEX:32008L0056:EN:HTML [accessed 15 August 2012].

Anonymous. 2013 Mareano website [online]. Available from http://www.mareano.no/en [accessed 9 April 2013].

Caldwell, J., and Dragoset, W. 2000. A brief overview of seismic air-gun arrays. The Leading Edge, **19**: 898–902. doi:10.1190/1.1438744.

Carey, W.M. 2006. Sound Sources and Levels in the Ocean. IEEE J. Oceanic Eng. **31**: 61–75. doi:10.1109/JOE.2006.872214.

De Robertis, A., and Handegard, N.O. 2013. Fish avoidance of research vessels and the efficacy of noise-reduced vessels: a review. ICES J. Mar. Sci. **70**: 34–45. doi:10.1093/icesjms/fss155.

Engås, A., Løkkeberg, S., Ona, E., and Soldal, A.V. 1993. Effects of seismic shooting on catch and catch availability of cod and haddock. Fisken og Havet, **9**.

Engås, A., Løkkeborg, S., Ona, E., and Soldal, A.V. 1996. Effects of seismic shooting on local abundance and catch rates of cod (*Gahus morhua*) and haddock (*Melanogrammus aeglefinus*). Can. J. Fish. Aquat. Sci. **53**(10): 2238–2249. doi:10.1139/f96-177.

Frid, A., and Dill, L.M. 2002. Human-caused disturbance stimuli as a form of predation risk. Conserv. Ecol. **6**: 11.

Del Grosso, V.A. 1974. New equation for the speed of sound in natural waters (with comparisons to other equations). J. Acoust. Soc. Am. **56**: 1084–1091. doi:10.1121/1.1903388.

Gytre, T. 1991. A new system for automatic STD data acquisition from randomly positioned observers. ICES CM 1991 C:21.

Hamilton, E.L. 1987. Acoustic properties of sediments. *In* Acoustics and ocean bottom. *Edited by* L. Lara-Sáenz, C. Ranz-Guerra, and C. Carbó-Fité. Consejo Superior de Invertigaciones Cientificas (C.S.I.C.), Madrid.

Hassel, A., Knutsen, T., Dalen, J., Skaar, K., Løkkeborg, S., Misund, O.A., Østensen, Ø., Fonn, M., and Haugland, E.K. 2004. Influence of seismic shooting on the lesser sandeel (*Ammodytes marinus*). ICES J. Mar. Sci. **61**: 1165–1173. doi:10.1016/j.icesjms.2004.07.008.

Heathershaw, A.D., Ward, P.D., and David, A.M. 2001. The environmental impact of underwater sound. *In* Proc. I.O.A., Vol. 23.

Hildebrand, J.A. 2009. Anthropogenic and natural sources of ambient noise in the ocean. Mar. Ecol. Progr. Ser. **395**: 5–20. doi:10.3354/meps08353.

Hovem, J.M. 2011. Ray trace modeling of underwater sound propagation [online]. Documentation and use of the PlaneRay model. SINTEF A21539. Available from http://www.sintef.no/Publikasjoner-SINTEF/Publikasjon/?pubid=SINTEF+A21539.

Hovem, J.M., Tronstad, T.V., Karlsen, H.E., and Lokkeborg, S. 2012. Modeling propagation of seismic airgun sounds and the effects on fish behavior. IEEE J. Oceanic Eng. **37**: 576–588. doi:10.1109/JOE.2012.2206189.

Jensen, F.B., Kuperman, W.A., Porter, M.B., and Schmidt, H. 2011. Computational ocean acoustics. Springer.

Lima, S.L., and Dill, L.M. 1990. Behavioral decisions made under the risk of predation: a review and prospectus. Can. J. Zool. **68**(4): 619–640. doi:10.1139/z90-092.

Løkkeborg, S., Ona, E., Vold, A., et al. 2010. Effekter av seismiske undersøkelser på fiskefordeling og fangstrater for garn og line i Vesterålen sommeren 2009. (Effects of seismic surveys on fish distribution and catch rates of gillnets and longlines in Vesterålen in summer 2009.) Fisken og Havet, **2-2010**.

Løkkeborg, S., Ona, E., Vold, A., and Salthaug, A. 2012. Sounds from seismic air guns: gear- and species-specific effects on catch rates and fish distribution. Can. J. Fish. Aquat. Sci. **69**(8): 1278–1291. doi:10.1139/f2012-059.

Madsen, P.T. 2005. Marine mammals and noise: Problems with root mean square sound pressure levels for transients. J. Acoust. Soc. Am. **117**: 3952–3957. doi:10.1121/1.1921508. PMID:16018497.

McCauley, R.D., Fewtrell, J., and Popper, A.N. 2003. High intensity anthropogenic sound damages fish ears. J. Acoust. Soc. Am. **113**: 638–642. doi:10.1121/1.1527962. PMID:12558299.

Milinski, M., Barnard, C.J., and Behnke, J.M. 1990. Parasites and host decision-making. *In* Parasitism and host behavior. *Edited by* C.J. Barand and J.M. Behnke. CRC Press, Boca Raton, Florida. pp. 95–116.

Pearson, W.H., Skalski, J.R., and Malme, C.I. 1992. Effects of sounds from a geophysical survey device on behavior of captive rockfish (*Sebastes* spp.). Can. J. Fish. Aquat. Sci. **49**(7): 1343–1356. doi:10.1139/f92-150.

Peña, H., Handegard, N.O., and Ona, E. 2013. Feeding herring schools do not react to seismic air-gun surveys. ICES J. Mar. Sci. [In press.] doi:10.1093/icesjms/fst079.

Popper, A.N., and Hastings, M.C. 2009. The effects of anthropogenic sources of sound on fishes. J. Fish Biol. **75**: 455–489. doi:10.1111/j.1095-8649.2009.02319.x. PMID:20738551.

Skalski, J.R., Pearson, W.H., and Malme, C.I. 1992. Effects of sounds from a geophysical survey device on catch-per-unit-effort in a hook-and-line fishery for rockfish (*Sebastes* spp.). Can. J. Fish. Aquat. Sci. **49**(7): 1357–1365. doi:10.1139/f92-151.

Slabbekoorn, H., Bouton, N., van Opzeeland, I., Coers, A., ten Cate, C., and Popper, A.N. 2010. A noisy spring: the impact of globally rising underwater sound levels on fish. Trends Ecol. Evol. **25**: 419–427. doi:10.1016/j.tree.2010.04.005. PMID:20483503.

Slotte, A., Hansen, K., Dalen, J., and Ona, E. 2004. Acoustic mapping of pelagic fish distribution and abundance in relation to a seismic shooting area off the Norwegian west coast. Fish. Res. **67**: 143–150. doi:10.1016/j.fishres.2003.09.046.

Tronstad, T.V., and Hovem, J.M. 2011. Model evaluation of Vesterålen and the Halten Bank [online]. SINTEF A17775. Available from http://www.sintef.no/home/Publications/Publication/?pubid=SINTEF+A17775.